



PERGAMON

Solid State Communications 117 (2001) 395–400

solid  
state  
communications

www.elsevier.com/locate/ssc

# Radiative lifetimes of single excitons in semiconductor quantum dots — manifestation of the spatial coherence effect

E. Dekel<sup>a</sup>, D.V. Regelman<sup>a</sup>, D. Gershoni<sup>a,\*</sup>, E. Ehrenfreund<sup>a</sup>,  
W.V. Schoenfeld<sup>b</sup>, P.M. Petroff<sup>b</sup>

<sup>a</sup>Department of Physics, Solid State Institute, Technion-Israel Institute of Technology, Haifa 32000, Israel

<sup>b</sup>Materials Department, University of California, Santa Barbara, CA 93106, USA

Received 9 November 2000; accepted 17 November 2000 by A. Pinzuk

## Abstract

Using time correlated single photon counting combined with temperature dependent diffraction limited confocal photoluminescence spectroscopy we accurately determine, for the first time, the intrinsic radiative lifetime of single excitons confined within semiconductor quantum dots. Their lifetime is one (two) orders of magnitude longer than the intrinsic radiative lifetime of single excitons confined in semiconductor quantum wires (wells) of comparable confining dimensions. We quantitatively explain this long radiative time in terms of the reduced spatial coherence between the confined exciton dipole moment and the radiation electromagnetic field. © 2001 Elsevier Science Ltd. All rights reserved.

**Keywords:** A. Semiconductor; A. Nanostructures; D. Electron–electron interactions; E. Luminescence; E. Time resolved optical spectroscopies

**PACS:** 78.66.Fd; 71.35.-y; 71.45.Gm; 85.30.Vw

In intrinsic direct bandgap semiconductors the interaction of excitons with the electromagnetic radiation field leads to a stationary state called exciton–polariton. This elementary excitation is a coherent state of the entire macroscopic three-dimensional (3D) crystal, and as such it does not decay radiatively [1]. In geometrically restricted semiconductor quantum structures such as quantum wells (QWs), wires (QWRs) or dots (QDs) the situation is different. In these systems, the translational symmetry of the crystalline potential is removed in one, two or three directions, respectively. As a result, the 3D electromagnetic radiation field interacts with excitons of lower dimensionality (2D, 1D or 0D, respectively). This dimensionality difference gives rise to exciton–polariton modes that are not stationary states. These modes have finite energy width,  $\Delta E$ , and consequently they do decay radiatively, [2–5] with intrinsic radiative lifetime  $\hbar/\Delta E$ , which, for typical GaAs/AlGaAs QWs, amounts to a few tens of picoseconds [4,6], while

for QWRs of comparable dimensions it is considerably longer [5,7,8]. This counter-intuitive result was explained in terms of the reduced exciton-coherence volume, imposed by the additional lateral confinement [2,5].

The arguments of this exciton–polariton theory explain also the considerably longer photoluminescence (PL) decay times which were measured in these systems [7–9]. They result from the thermal distribution of the excitonic population, where only a small fraction occupies the optically active part of the available excitonic phase space [4,5]. Consequently, the dimensional dependent density of energy states reveals itself in the temperature dependence of the radiative decay times. Indeed, both theory and experiment show that these are proportional to the temperature,  $T$ , in QWs [4,9] and to  $\sqrt{T}$  in QWRs [5,7,8]. When these considerations are applied to QDs, longer intrinsic radiative lifetimes are expected [10], and their characteristic  $\delta$ -function like density of energy states leads to  $T$  independent radiative decay times. Though numerous experimental studies of the PL decay times from QD assemblies [11,12] and more recently from single QDs [13–15], have already been carried out, this theoretically expected behavior has never been observed.

\* Corresponding author. Tel.: +972-4-8293693;  
fax: +972-4-8235107.

E-mail address: ssrdgdg@ssrc.technion.ac.il (D. Gershoni).

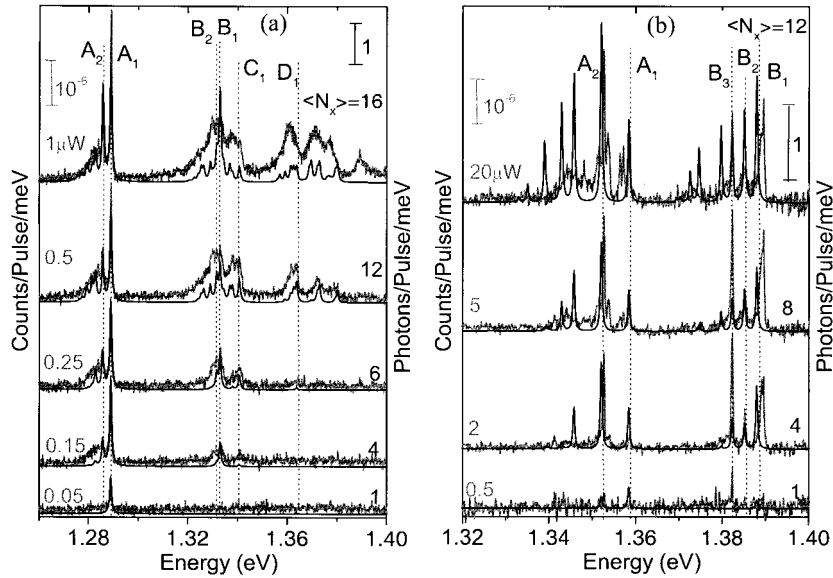


Fig. 1. (a) and (b) PL spectra from a single SAQD from the PCI(AHL) sample for various pulsed excitation powers. The gray lines and right axes represent our model simulations.

In this letter we report on the first experimental determination of the radiative lifetime of single excitons confined within semiconductor QDs. We determine this fundamental property of 0D excitons by applying time correlated single photon counting combined with confocal microscopy to single self-assembled quantum dots (SAQDs). The temporal evolution of the PL emission following pulse excitation at various intensities is measured and the PL intensity is quantitatively analyzed taking into account the interaction between a number of excitons (multiexcitons) confined within one QD [16–18]. Our intensity and temporal analysis unambiguously determine the intrinsic radiative lifetime of single QD excitons. We show that they are few nanoseconds (ns) long and  $T$  independent.

We studied two types of SAQDs. Both were fabricated by molecular beam epitaxial deposition of a defect free coherently strained epitaxial layer of InAs on either directly on a GaAs layer by the partially covered islands method [19] (PCI sample) or on an AlGaAs host layer (AHL sample) [16]. The layer sequences, compositions and widths are reported elsewhere [16,19]. During the growth of the strained layers, the samples were not rotated. Thus, a gradient in the QDs density was formed and low-density areas, in which the average distance between neighboring QDs is larger than the spatial resolution of our microscope were found on their surfaces. A key difference between the two samples is their non-radiative decay rates. The presence of Al within the SAQDs' host layers of the AHL sample gives rise to very efficient non-radiative recombination centers [20], close to the SAQDs. Therefore, at low excitation densities their PL decay time is extremely short [17]. It is shown below that in spite of this difference, the determined

radiative lifetimes of single excitons in both samples are roughly the same, as expected from the dimensional considerations.

The PL was excited by a synchronously mode-locked 3 ps pulsed dye-laser through a low temperature confocal microscope, which is described elsewhere [17]. The system provides spectral and spatial resolutions of 0.2 meV and  $\approx 0.5 \mu\text{m}$ , respectively. In addition, a thermoelectrically cooled avalanche silicon photodiode was used for photon counting with temporal resolution of 200 ps.

In Fig. 1(a) and (b) we present by solid lines temporally integrated PL spectra from a single PCI (AHL) SAQD for various  $\geq 1.75$  eV pulsed excitation powers. At the lowest power PL spectrum of Fig. 1(a) a single narrow spectral line is observed at energy of 1.284 eV. We denote this line by  $A_1$ . Its linewidth is limited by our setup resolution. As the excitation power increases, a satellite spectral line ( $A_2$ ) appears 3.5 meV below  $A_1$  and a higher energy spectral line, ( $B_1$ ) emerges at 1.324 eV, 40 meV above  $A_1$ . At yet higher excitation power line  $B_1$  develops a 1.5 meV lower in energy satellite ( $B_2$ ). Further increase in the excitation power results in an increase in the number of satellites which gradually form spectral emission bands to the lower energy side of the lines  $A_1$  and  $B_1$ . In addition, new higher energy groups of lines, C, D and E, respectively, gradually emerge and develop their own satellites and lower energy bands. The various lines are marked by letters, which represent the energy group to which they belong and numerical subscripts, which represent their appearance order with increasing the excitation power. As the power increases, after reaching maximum, the intensity of the emission from the various spectral lines ceases to increase and it

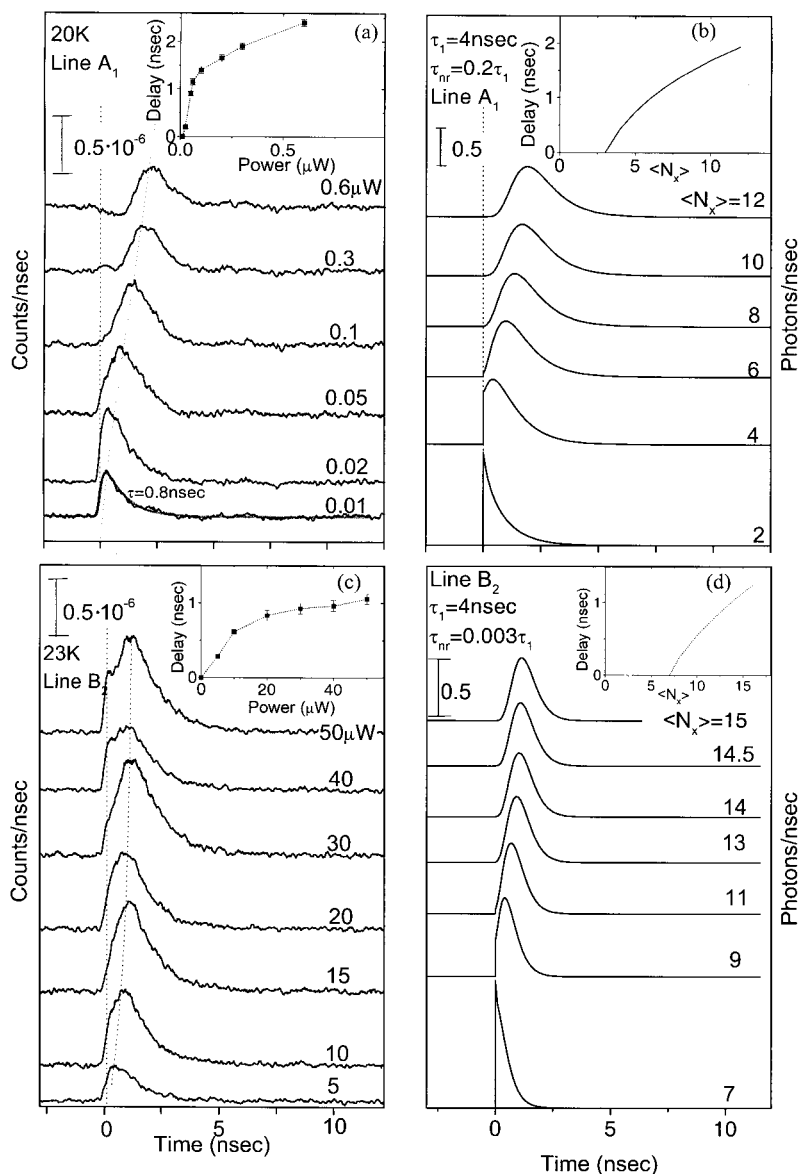


Fig. 2. The intensity of line A<sub>1</sub>(B<sub>2</sub>) from a single SAQD of the PCI(AHL) sample vs. time after the excitation pulse measured (a), (c) for various excitation powers and calculated (b), (d) for various average number of photogenerated QD excitons,  $\langle N_x \rangle$ . The insets to (a) and (c) (b) and (d) display the measured (calculated) rise times of the PL, vs. excitation power ( $\langle N_x \rangle$ ).

remains constant with further increase in the power. This is in marked difference from their behavior under continuous wave (cw) excitation mode, where they gradually disappear [17,18].

The behavior of the PL spectra from the AHL sample (Fig. 1(b)) is similar, except for two major differences: First, only two groups of lines, A and B, are observed. Second, the satellite spectral line A<sub>2</sub> appears before the line A<sub>1</sub>. We explain the first difference by the different dimensions of the two dots. Whereas the first, larger one, has 4–5 confined electron levels, the second one has only

two. The second difference is due to the efficient non-radiative decay process associated with the Al atoms in the AHL sample. At low excitation densities, before it is saturated [17], it inhibits the observation of the line A<sub>1</sub>. Our model simulations [17,18] are presented in the figures by gray lines.

In Fig. 2(a) and (c) we present the PL intensity of the single SAQD spectral line A<sub>1</sub>(B<sub>2</sub>) from the PCI(AHL) sample as a function of time after the excitation pulse. The PL transients were measured at 20 K for various excitation powers. In general, for each spectral line there are two

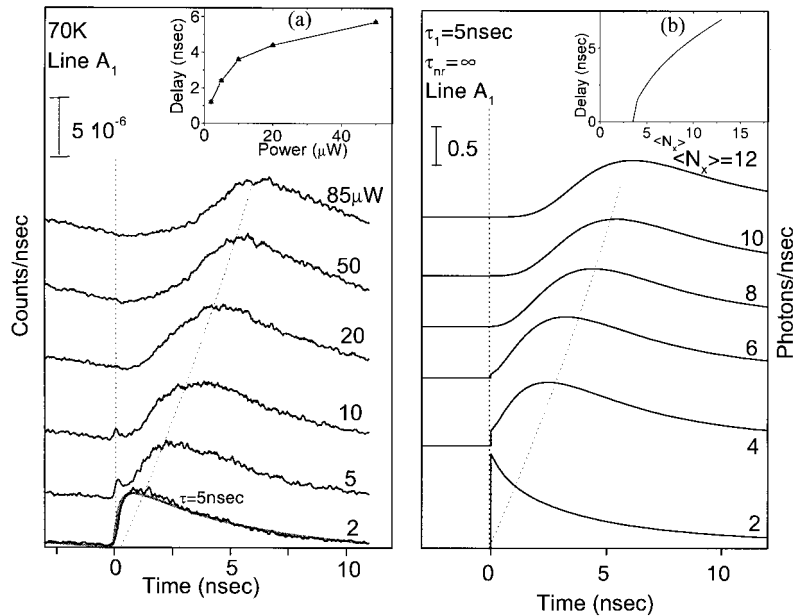


Fig. 3. The intensity of line A<sub>1</sub> from SAQD from the PCI sample vs. time at 70 K (a), (b) Measured (calculated) for various powers ( $\langle N_x \rangle$ , values). The inset display the measured (calculated) rise time of the PL vs. the excitation power ( $\langle N_x \rangle$ ).

distinct time domains. In the first, the emission intensity rises and in the second, it decays. As a rule we noted (not shown) that the lower is the energy of a given spectral group of lines, the longer are their rise and decay times. Within a given group of lines, however, lower energy lines rise and decay faster. Our model calculations [17,18] for the A<sub>1</sub>(B<sub>2</sub>) line of the PCI(AHL) sample are presented for comparison in Fig. 2(b) and (d). Clearly, the rise time of a particular spectral line, strongly depends on the excitation power. The higher the power is, the longer is the rise time, while the decay time is hardly affected. We note that the temporal behavior of the spectral lines from the different samples is very similar. The main difference is the density of excitation needed to observe the PL from the second sample. This difference, like the difference in the order by which the spectral lines appear with increasing excitation power is explained by the vast efficiency difference between the non-radiative recombinations in the two samples. In the inset to Fig. 2(a) and (c) we display by symbols the measured rise time of the spectral line A<sub>1</sub>(B<sub>2</sub>), as a function of the excitation power. Our model calculations are presented for comparison in the inset to Fig. 2(b) and (d). Similar measurements and calculations are presented in Fig. 3(a) and (b), respectively, for the spectral line A<sub>1</sub> of an SAQD from the PCI sample, at higher sample temperature of 70 K.

The PL spectrum of a semiconductor QD excited by a short laser pulse is due to optical transitions between multiexciton states [17,18]. The excitation generates population of electron–hole (e–h) pairs within the dot. The many e–h pairs from a correlated quantum state which we define as a multiexciton. The photoexcited carriers reach thermal

distribution on a very short time scale compared with the time required for radiative recombination of an e–h pair. Thus, at cryogenic temperatures, the specific excited multiexciton rapidly relaxes to its ground level. A radiative annihilation of one of the e–h pairs that compose the multiexciton may then occur by the emission of a photon, which carries the energy difference between the annihilated multiexcitonic ground level and that of the newly generated one. The new multiexciton, with one less e–h pair quickly relaxes to its ground level and eventually recombines by losing yet another e–h pair. The process continues sequentially, until the dot remains empty of excitons. For a small number of QD excitons ( $\leq 2$ ), the probability of non-radiative recombination becomes increasingly important. First, since the non-radiative decay channels are no longer screened by the carriers in the QD and its vicinity. Second, since the radiative recombination has fewer channels and its rate is much slower [17,18].

In order to understand the spectral evolution of the SAQD PL with excitation power and with time, a knowledge of the various multiexcitons energies and recombination rates is required. Our model provides a straightforward way for calculating these energies using a minimal set of parameters (i.e. the single carrier energy levels and the exchange energies between these levels), which can be obtained directly from the PL spectrum itself [17,18]. The recombination rates are given by the model in terms of the QD single exciton radiative lifetime ( $\tau_1$ ) through the use of the dipole approximation, together with symmetry and total angular momentum conservation considerations. These energies and rates are used for calculating the spectra in Fig. 1,

where a Gaussian spectral broadening of 0.5 meV for each discrete multiexcitonic level was used, and the statistical nature of the pulse photogeneration was taken into account. Thus,  $\langle N_X \rangle$  in Fig. 1 represents the average number of photo-generated pairs (or the multiexciton order) in the QD by each laser pulse. Since the spectra in Fig. 1 are temporally integrated, each multiexciton of order  $\leq N_X$  contributes exactly one radiative recombination to the measured spectrum. From this simple argument, it follows that the comparison between the calculated spectra of Fig. 1 and the measured spectral density of counts per pulse at saturation, directly yields the collection efficiency of our setup. This calculated number is almost model independent since the number of photons per recombination is easily obtained from total spin conservation considerations [16–18,21]. The efficiency obtained from Fig. 1,  $\approx 5 \times 10^{-5}$ , does not depend on the efficiency of excitation or on the non-radiative processes and it is in very good agreement with our estimates based on measuring the reflected laser light.

We use the multiexcitons calculated recombination rates as input parameters to a set of coupled rate equations which describe the temporal behavior of the pulsed photoexcited single QD. The rate equations are analytically solved for the CW and pulsed excitation modes [17,18]. The cw solution yields a direct determination of the radiative lifetime  $\tau_1$ . For this task one uses the determined efficiency of the experimental system and the cw excitation power dependence of the PL spectrum. As mentioned above, when the cw excitation power increases the various SAQD PL discrete spectral lines reach maximum emission and then lose intensity with further increase in the power (not shown) [16–18]. The steady-state number of QD excitons when a certain line reaches maximum is thereby given by comparison with the analytic solution of the rate equations. The calibrated emission intensity at these conditions, accurately determines  $\tau_1$  [17,18].

Another independent way of determining  $\tau_1$  is demonstrated by the curves in Fig. 2(b) and (d), which represent the solution to the rate equations of the pulsed excitation mode. Two parameters are used for generating all the simulated transient curves. Namely,  $\tau_1$  and the ratio between it and the non-radiative lifetime ( $\tau_{nr}$ ). From the comparison between the measured data (Fig. 2(a) and (c) and their insets) and the calculated ones (Fig. 2(b) and (d) and their insets) we find that the best fit for the PCI sample is obtained when  $\tau_1/\tau_{nr} \approx 5$ . For this and higher ratios,  $\tau_{nr}$  can be directly obtained from the PL decay time of  $A_1$ , which exponentially decays within  $0.8 \pm 0.1$  ns ( $\tau$  in Fig. 2(a)). Consequently,  $\tau_1$  that we deduced for the PCI SAQDs at this temperature is  $4 \pm 1$  ns, in very good agreement with its PL efficiency determination [17,18].

We state here that the determination of  $\tau_1$  is not very sensitive to  $\tau_{nr}$  since it is determined mainly from the power dependence of the rise time. Thus, variations in  $\tau_1/\tau_{nr}$  ratio from zero to almost infinity yields only up to a factor of two change in the deduced  $\tau_1$ . Similarly, we

determined  $\tau_1$  of the AHL SAQDs to be  $5 \pm 1$  ns, and more than 2 orders of magnitude longer than their  $\tau_{nr}$ .

The decay time of the PL in the PCI sample is found to rapidly increase with  $T$ , while the rise time hardly changes. This is evident from the PL decay time of the  $A_1$  line at 70 K ( $\tau$  in Fig. 3(a)), which is  $5 \pm 1$  ns long. We believe that this is due to reduction in the non-radiative rate due to thermal activation of trapped charges that act as non-radiative centers in the vicinity of the SAQD. The best fits in Fig. 3b were obtained with  $\tau_1/\tau_{nr} \ll 1$ . This means that at this temperature the non-radiative rate can be neglected, and the radiative time which determines the PL rise time, now determines its decay time as well. The AHL sample non-radiative rates are activated with increasing  $T$  and they become even faster [20]. They render the temporal resolution of the emission from discrete PL lines at elevated  $T$ , nearly impossible.

The lifetime that we obtain for both samples, using these two independent experimental methods, amounts to 4–6 ns, and it is temperature independent. This is much longer than the measured PL decay times from single SAQDs [13–15] and from SAQD assemblies [11,12], where typically, like here, low temperature sample dependent decay times of subnanosecond are reported. We show here that this is because at low excitation densities the decay time depends crucially on the non-radiative recombinations, while at high excitation densities one measures faster decays of multiexcitons. Our approach, which is independent of the measured PL decay time, clearly circumvent these impediments. We demonstrated that only at 70 K, when the non-radiative decay process of the PCI sample is blocked, the PL decay is purely radiative and  $\tau_1$  can be directly obtained from its measurement. We also demonstrated that even for the QDs in the AHL sample long radiative lifetimes are deduced, in spite of their very fast non-radiative decay rates.

The QD single exciton radiative lifetime is much longer than the intrinsic radiative time of higher dimensional systems such as wires [5,7,8] and wells [4,6,9]. Following the arguments of Andreani [4], and Citrin [5] who calculated the intrinsic radiative lifetimes of single excitons in semiconductor QWs and QWRs, respectively, we find for excitons in spherical QDs:

$$\tau_0^{\text{QD}} = nm_0c/e^2fk_{\text{ex}}^2, \quad (1)$$

where  $n$ ,  $m_0$ ,  $e$  and  $c$  are the material index of refraction, electronic mass, electron charge and speed of light, respectively,  $f$  is the confined exciton oscillator strength and  $k_{\text{ex}} = n\omega/c$  is the exciton wavevector in the material. For exciton energy  $\hbar\omega = 1.35$  eV and  $f = 0.5$  for QDs of these dimensions [22], we get  $\tau_0^{\text{QD}} = 4.2$  ns, in reasonable agreement with our temperature independent experimental findings. We therefore conclude that the long QDs single exciton radiative lifetimes that we measured are due to the small spatial phase coherence between the 3D confined excitonic dipole and the electromagnetic radiation field in the semiconductor matter.

**Acknowledgements**

The work was supported by the Israel Science Foundation and by the Israel–US Binational Science Foundation.

**References**

- [1] J.J. Hopfield, *Phys. Rev.* 112 (1958) 1555.
- [2] V.M. Agranovitch, A.O. Dubovskii, *JETP Lett.* 3 (1996) 223.
- [3] E. Hanamura, *Phys. Rev. B* 38 (1988) 1228.
- [4] L.C. Andreani, *Solid State Commun.* 77 (1991) 641.
- [5] D.S. Citrin, *Phys. Rev. Lett.* 69 (1992) 3393.
- [6] B. Devaud, et al., *Phys. Rev. Lett.* 67 (1991) 2355.
- [7] H. Akiyama, et al., *Phys. Rev. Lett.* 72 (1994) 924.
- [8] D. Gershoni, et al., *Phys. Rev. B* 50 (1994) 8932.
- [9] J. Feldman, et al., *Phys. Rev. Lett.* 59 (1987) 2337.
- [10] D.S. Citrin, *Superlattice Microstruct.* 13 (1993) 303.
- [11] S. Grosse, et al., *Phys. Rev. B* 55 (1997) 4473.
- [12] J. Bellessa, et al., *Phys. Rev. B* 58 (1998) 9933.
- [13] U. Bockelmann, et al., *Phys. Rev. Lett.* 76 (1996) 3622.
- [14] G. Bacher, et al., *Phys. Rev. Lett.* 83 (1999) 4417.
- [15] V. Zwiller, et al., *Phys. Rev. B* 59 (1999) 5021.
- [16] E. Dekel, et al., *Phys. Rev. Lett.* 80 (1998) 4991.
- [17] E. Dekel, et al., *Phys. Rev. B* 61 (2000) 11009.
- [18] E. Dekel, et al., *Phys. Rev. B* 62 (2000) 11038.
- [19] J.M. Garcia, et al., *Appl. Phys. Lett.* 72 (1998) 3172.
- [20] I. Shtrichman, D. Gershoni, R. Kalish, *Phys. Rev. B* 56 (1997) 1509.
- [21] A. Williamson, A. Franceschetti, A. Zunger, *cond-mat/0003188*.
- [22] T. Takagahara, *Phys. Rev. B* 39 (1989) 10206.